J. Austral. Math. Soc. Ser. B 40(1998), 97–122

AN ANALYSIS OF LOCAL ENERGY AND PHASE CONGRUENCY MODELS IN VISUAL FEATURE DETECTION

Y. K. AW[1], ROBYN OWENS[1] and JOHN ROSS[2]

(Received 29 November 1994; revised 30 January 1996)

Abstract

A variety of approaches have been developed for the detection of features such as edges, lines, and corners in images. Many techniques presuppose the feature type, such as a step edge, and use the differential properties of the luminance function to detect the location of such features. The local energy model provides an alternative approach, detecting a variety of feature types in a single pass by analysing order in the phase components of the Fourier transform of the image. The local energy model is usually implemented by calculating the envelope of the analytic signal associated with the image function. Here we analyse the accuracy of such an implementation, and show that in certain cases the feature location is only approximately given by the local energy model. Orientation selectivity is another aspect of the local energy model, and we show that a feature is only correctly located at a peak of the local energy function when local energy has a zero gradient in two orthogonal directions at the peak point.

1. Introduction

Images are spatial data patterns, normally represented as bounded and sampled luminance values over a bounded and sampled two-dimensional spatial domain. One of the major problems in image analysis is the detection of image features such as edge and corner points, since it is well-accepted that such features contain much of the information in the image, and occur on a set of small measure. Many approaches have been developed for the detection and localisation of features, including differential techniques [5, 10, 19], surface-fitting techniques [7, 8], morphological approaches [14] and others [21].

Accurate feature detection is essential for many of the problems currently facing researchers in the field of *active vision*, especially with regards to stereo, motion

[1]Department of Computer Science, The University of Western Australia, Nedlands, WA 6907
[2]Department of Psychology, The University of Western Australia, Nedlands, WA 6907

analysis, and hand-eye coordination in robotics. Moreover, Oppenheim and Lim [15] showed in 1981 that *phase* information is crucial to our perception of features, and Fleet and Jepson [6] have used phase information to extract motion in images.

Morrone and Owens (1987) approach the problem of feature detection by considering how features are built up in an image instead of the differential properties in the luminance function. They proposed the phase congruency model for feature detection. In their approach an image is decomposed into its frequency components. A feature point is marked at the spatial location where the phases of frequency components in a particular direction are maximally congruent in a local neighbourhood. They also hypothesize that feature points located by the phase congruency criterion coincide with those perceived by the human visual system [11, 12], including some illusory features like Mach bands [13].

The concept of maximal congruency in phase entails the minimisation of some measure of error. Various error functions can be used. However, instead of using an error function, Morrone and Owens implement phase-congruency by defining a local energy function. Features are said to be found at points where the local energy function peaks. The local energy function is defined as the norm of an energy vector whose two bases are the image itself and its Hilbert transform. To tie in with the original idea of localizing features at points of maximal phase congruency, they define a "phase-congruency" function as the scaled version of the local energy function, the scaling factor being the sum of the amplitudes of all frequency components. By such definitions, the maximisation of the local energy function naturally maximises the phase-congruency function. In this paper, a weighted least-square error function (as one of the many possible ways to measure "congruency") is defined for the deviation in component phase angles and must be minimised to mean *phase-congruency*. It is shown in Section 4 that the local energy model is a Taylor approximation of the weighted least-square method in implementing phase congruency.

In this paper we will restrict the analysis of the model to one-dimensional image signals. However, the local energy model has been implemented for the analysis of two-dimensional images [22]. The implementation involves convolving the image signal with quadrature pairs of filters, one of which is rotationally symmetric and the other orientationally selective. The phase congruency model has also been implemented using banks of wavelet filters [9] and extended for the detection of two-dimensional features such as corners and junctions [20]. Some of the mathematical properties of the model have been detailed in our previous work [1–4, 11, 12, 16–18, 23], but this paper represents the first detailed analysis of the model's accuracy.

The orientation invariance property of the phase congruency and the local energy models is also examined. Features in an image can exist in any direction. In the event of 1-D feature points forming a curve, the ideal implementation of a feature detector should be operating in a direction normal to the feature curve at each point.

Indeed, this is how Canny's operator detects step edges. However, many feature detectors, including early versions of the local energy model, are one-dimensional if implementation is to be simple and efficient [22]. The outputs of the feature detector in two orthogonal directions are often summed to represent a two-dimensional detection. Although it has been empirically demonstrated that reasonable results can be obtained in such a manner by the local energy model [22], a mathematical analysis has not been provided. This paper provides the proof that the location of the peaks of local energy, or locations of minimal weighted least-square phase error, remain invariant regardless of the chosen directions of the two bases of operation, provided some conditions are met. These are discussed in Section 6.

2. The local energy model

The following discussion will be restricted to one-dimensional analog signals $f(x)$. The image, I, that such a signal represents is the two-dimensional array of points $\{I(x, y) = f(x)$, where x and y are in some interval$\}$. That is, $f(x)$ represents a horizontal slice through the image $I(x, y)$ and such slices are identical, regardless of the choice of y. One can imagine a simple step edge image, with a black panel on the left-hand side, and a white panel on the right.

Let a one-dimensional zero-dc luminance function $f(x)$ be defined in terms of its Fourier frequency components as

$$f(x) = 2\sum_{n>0} a_n \cos(n\omega x + \phi_n), \tag{2.1}$$

where a_n and ϕ_n are the amplitude and phase of the n^{th} frequency component respectively.

Let the Hilbert Transform of $f(x)$ be $h(x)$. Then, by definition of the Hilbert transform,

$$h(x) = -2\sum_{n>0} a_n \sin(n\omega x + \phi_n). \tag{2.2}$$

An energy vector can be defined as

$$\begin{aligned} e(x) &= \frac{1}{2}[f(x), -h(x)] \\ &= \left[\sum_{n>0} a_n \cos(n\omega x + \phi_n), \sum_{n>0} a_n \sin(n\omega x + \phi_n)\right]. \end{aligned} \tag{2.3}$$

The local energy function [22], E, is defined as the norm of the vector $e(x)$:

$$E(x) = \sqrt{\left[\sum_{n>0} a_n \cos(n\omega x + \phi_n)\right]^2 + \left[\sum_{n>0} a_n \sin(n\omega x + \phi_n)\right]^2}. \tag{2.4}$$

https://doi.org/10.1017/S0334270000012406 Published online by Cambridge University Press

Alternatively, $E(x)$ can be expressed as

$$E(x) = \sum_{n>0} a_n \cos(n\omega x + \phi_n - \theta_e), \tag{2.5}$$

where

$$\theta_e = \tan^{-1}\left(\frac{\sum_{n>0} a_n \sin(n\omega x + \phi_n)}{\sum_{n>0} a_n \cos(n\omega x + \phi_n)}\right). \tag{2.6}$$

Equation (2.5) is derived by summing the dot-products of all frequency component vectors with a unit vector along $e(x)$. The value E (2.4) is the norm of the resultant vector e of all the components using the Cartesian coordinates, where $n\omega x + \phi_n = 0$ is the x-axis (and $\pi/2$ is the y-axis). But if the component vectors are summed using other Cartesian coordinates where $n\omega x + \phi_n - \theta_e = 0$ is the x-axis (and $\pi/2$ is the y-axis), that is, using the e direction as the x-axis, then the same e should be obtained as before (because the vector sum is independent of the coordinate system used) and the e in the latter coordinate system is real (zero imaginary part) giving E directly (2.5).

Alternately, the identity of (2.4) and (2.5) can also be proven as follows.

The norm (E) of a vector (e) is the dot product of the vector (e) with its unit vector ($\hat{e}$) along the same direction:

$$\begin{aligned} E &= e \bullet \hat{e} \\ &= \left[\sum_{n>0} a_n \cos(n\omega x + \phi_n) \quad \sum_{n>0} a_n \sin(n\omega x + \phi_n)\right] \begin{bmatrix}\cos(\theta_e) \\ \sin(\theta_e)\end{bmatrix} \\ &= \sum_{n>0} a_n \cos(n\omega x + \phi_n)\cos(\theta_e) + \sum_{n>0} a_n \sin(n\omega x + \phi_n)\sin(\theta_e) \\ &= \sum_{n>0} a_n \cos(n\omega x + \phi_n - \theta_e). \end{aligned}$$

Next, that E is maximised at θ_e given any x before finding peaks of E with respect to x will be ascertained.

THEOREM 1. *The value of θ in the function*

$$p(x, \theta) = \sum_{n>0} a_n \cos(n\omega x + \phi_n - \theta)$$

must be equal to θ_e (2.6) if p is to be maximised at any given x.

https://doi.org/10.1017/S0334270000012406 Published online by Cambridge University Press

PROOF. We have

$$\frac{\partial p}{\partial \theta} = \sum_{n>0} a_n \sin(n\omega x + \phi_n - \theta), \tag{2.7}$$

$$\frac{\partial^2 p}{\partial \theta^2} = -\sum_{n>0} a_n \cos(n\omega x + \phi_n - \theta) = -p.$$

Since p is non-negative (being the norm of a vector (see equation (2.5)), extrema of p (with respect to θ, not x), if any, must be maxima, not minima. To find θ at maxima of p given x, set $\frac{\partial p}{\partial \theta}$ (2.7) to zero. Then

$$\sum_{n>0} a_n \sin(n\omega x + \phi_n - \theta) = 0,$$

$$\sum_{n>0} a_n[\sin(n\omega x + \phi_n)\cos(\theta) - \cos(n\omega x + \phi_n)\sin(\theta)] = 0,$$

$$\cos(\theta)\sum_{n>0} a_n \sin(n\omega x + \phi_n) = \sin(\theta)\cos(n\omega x + \phi_n),$$

$$\theta = \tan^{-1}\left(\frac{\sum_{n>0} a_n \sin(n\omega x + \phi_n)}{\sum_{n>0} a_n \cos(n\omega x + \phi_n)}\right) = \theta_e.$$

By Theorem 1, it is known that the local energy E, at a given spatial location x, is maximised at the phase angle θ_e of the energy vector e, which is computed by standard vector algebra (2.6). This is to be contrasted with the statement [22] that says E is maximised at the weighted average of the component phases $\sum_{n>0} a_n(n\omega x + \phi_n)/\sum_{n>0} a_n$. (It will be shown that this is a Taylor's Series approximation.)

At θ_e, it is now desired to find x_e (the spatial location where $E(x, \theta)$ is maximised). To maximise E is to maximise the square of E (since E is non-negative). Thus, using (2.4), a function $Z(x)$ is defined as

$$Z(x) = \left[\sum_{n>0} a_n \cos(n\omega x + \phi_n)\right]^2 + \left[\sum_{n>0} a_n \sin(n\omega x + \phi_n)\right]^2. \tag{2.8}$$

Because of the identity of the expressions in (2.4) and (2.5), it is implicit that $\theta = \theta_e$ when $Z(x)$ is defined as in (2.8). We have

$$\frac{\partial Z}{\partial x} = -2\left[\sum_{n>0} a_n \cos(n\omega x + \phi_n)\right]\left[\sum_{n>0} a_n n\omega \sin(n\omega x + \phi_n)\right]$$

https://doi.org/10.1017/S0334270000012406 Published online by Cambridge University Press

$$+2\left[\sum_{n>0} a_n \sin(n\omega x+\phi_n)\right]\left[\sum_{n>0} a_n n\omega \cos(n\omega x+\phi_n)\right]$$
$$=2\sum_{m,n>0}(m-n)a_m a_n \sin(m\omega x+\phi_m)\cos(n\omega x+\phi_n).$$

Setting $\partial Z/\partial x = 0$ gives

$$\sum_{m,n>0}(m-n)a_m a_n \sin(m\omega x_e+\phi_m)\cos(n\omega x_e+\phi_n)=0. \tag{2.9}$$

Equation (2.9) can be solved for x_e by numerical methods. For each x_e found, the usual second derivative test ($\partial^2 Z/\partial x^2 < 0$ for maxima) can be carried out. In summary, $E(x)$ peaks at the spatial location $x = x_e$ (2.9) with a phase angle $\theta = \theta_e$ (2.6).

3. Phase congruency via phase deviation

Next, the notion of phase-congruency will be studied. As a convenient example, a weighted least-square error function is defined to measure 'phase-congruency'. Let $r(x,\theta)$, a *phase deviation* function (rather than a 'phase-congruency' function [22]), be defined as

$$r(x,\theta)=\frac{\sum_{n>0} a_n (n\omega x+\phi_n-\theta)^2}{\pi^2 \sum_{n>0} a_n}, \tag{3.1}$$

where $n\omega x+\phi_n-\theta$ assumes values in the principal range $(-\pi,\pi]$.

The value of r will be in the closed interval [0.0, 1.0]. *Maximum phase congruency* means minimum phase deviation. Also note that by shifting $\omega x+\phi_n-\theta$ into the principal range of $(-\pi,\pi]$, mod (2π) computation is performed in (3.1).

As before, it is desired to find θ that minimises r at any given x before considering minimising r with respect to x.

THEOREM 2. *The value of θ in the function*

$$r(x,\theta)=\frac{\sum_{n>0} a_n (n\omega x+\phi_n-\theta)^2}{\pi^2 \sum_{n>0} a_n}$$

must be equal to the weighted average phase

$$\theta_r=\frac{\sum_{n>0} a_n (n\omega x+\phi_n)}{\sum_{n>0} a_n}$$

if r is to be minimised at any given x.

https://doi.org/10.1017/S0334270000012406 Published online by Cambridge University Press

PROOF. We have

$$\frac{\partial r}{\partial \theta} = \frac{-2}{\pi^2 \sum_{n>0} a_n} \sum_{n>0} a_n(n\omega x + \phi_n - \theta),$$

$$\frac{\partial^2 r}{\partial \theta^2} = \frac{2}{\pi^2 \sum_{n>0} a_n} \sum_{n>0} a_n > 0.$$

Since $\partial^2 r/\partial\theta^2 > 0$, any extrema of r must be minima.
Setting $\partial r/\partial\theta = 0$ (to find θ_r) gives

$$\sum_{n>0} a_n(n\omega x + \phi_n - \theta_r) = 0,$$

$$\sum_{n>0} a_n(n\omega x + \phi_n) - \sum_{n>0} a_n\theta_r = 0,$$

$$\theta_r = \sum_{n>0} a_n (n\omega x + \phi_n) \Big/ \sum_{n>0} a_n.$$

Note that the expression for θ_r in Theorem 2 is identical to the weighted average phase mentioned by Venkatesh [22]. What this means is that at θ_r, the local energy *does not* peak in general; instead, the phase deviation function *is* minimised.

Also note that special care must be taken when computing θ_r in mod (2π). One way is to separate $(n\omega x + \phi_n)$ into two groups: $(0, \pi]$ and $(-\pi, 0]$; compute a sub-weighted-average value in each group, and then combine the two sub-weighted-average values using the smaller angle of difference between them.

By Theorem 2, it is known that at the weighted average phase angle θ_r, the phases of the fourier components have weighted least square error (with respect to θ). Next, we compute the spatial location x_r where $r(x, \theta)$ is minimised. This is done by setting $\partial r/\partial x$ to 0 at $\theta = \theta_r(x)$. We have

$$r(x, \theta_r) = \frac{\sum_{n>0} a_n (n\omega x + \phi_n - \theta_r)^2}{\pi^2 \sum_{n>0} a_n},$$

$$\frac{\partial r}{\partial x} = \frac{2}{\pi^2 \sum_{n>0} a_n} \sum_{n>0} \left[a_n (n\omega x + \phi_n - \theta_r) \left(n\omega - \frac{\partial \theta_r}{\partial x} \right) \right]. \tag{3.2}$$

From Theorem 2,

$$\theta_r = \frac{\sum_{n>0} a_n (n\omega x + \phi_n)}{\sum_{n>0} a_n} = \omega M x + N,$$

https://doi.org/10.1017/S0334270000012406 Published online by Cambridge University Press

where

$$M = \sum_{n>0} a_n n \Big/ \sum_{n>0} a_n, \qquad N = \sum_{n>0} a_n \phi_n \Big/ \sum_{n>0} a_n,$$

and $\partial\theta_r/\partial x = \omega M$.

Therefore,

$$\frac{\partial r}{\partial x} = \frac{2}{\pi^2 \sum_{n>0} a_n} \sum_{n>0} [a_n(n\omega x + \phi_n - \omega M x - N)(n\omega - \omega M)] .$$

Setting $\partial r/\partial x = 0$ (to find x_r) gives

$$\sum_{n>0} [a_n(n\omega x_r + \phi_n - \omega M x - N)(n\omega - \omega M)] = 0. \tag{3.3}$$

Equation (3.3) is implicit with respect to x_r, and the expression $(n\omega x + \phi_n - \omega M x - N)$ cannot be separated to give

$$x_r = \frac{\sum_{n>0} [a_n(n - M)(N - \phi_n)]}{\omega \sum_{n>0} [a_n(n - M)]} \tag{3.4}$$

because for every x_r and n, $(n\omega x + \phi_n - \omega M x - N)$ must undergo mod (2π) arithmetic to assume values in $(-\pi, \pi]$. Numerical methods can be used to solve for x_r in (3.3) by looking for the zero-crossings.

In summary, phases of the harmonics are maximally congruent at location x_r with a phase angle value θ_r (3.3).

4. Phase congruency approximated by local energy peaks

We have shown that the local energy peaks at location x_e with phase value θ_e but phases of harmonics are maximally congruent at location x_r with phase value θ_r (in a weighted least-square sense). To say that local energy peaks at maximum phase congruency would mean $x_e = x_r$ and $\theta_e = \theta_r$. This happens only when all harmonics' phases $(n\omega x + \phi_n)$ are equal to θ_e. In vectorial terms, all the vectors representing each harmonic of the image at x_e will have to point in the same direction as the energy vector e does. The closer the harmonics' phases are to θ_e, the better the approximation of (x_r, θ_r) by (x_e, θ_e). This approximation is also known as the Taylor approximation. Proofs are provided below as Theorem 3 and 4.

THEOREM 3. *The energy phase value θ_e is approximately equal to the weighted phase value θ_r if all harmonics' phases $(n\omega x + \phi_n)$ are close to θ_e. (That is, $\theta_e \approx \theta_r$ if $n\omega x + \phi_n - \theta_e \approx 0$.)*

https://doi.org/10.1017/S0334270000012406 Published online by Cambridge University Press

PROOF. From (2.5),

$$E(x) = \sum_{n>0} a_n \cos(n\omega x + \phi_n - \theta_e),$$

$$\frac{\partial E}{\partial \theta_e} = \sum_{n>0} a_n \sin(n\omega x + \phi_n - \theta_e)$$
$$\approx \sum_{n>0} a_n (n\omega x + \phi_n - \theta_e) \quad \text{if } n\omega x + \phi_n - \theta_e \approx 0 \text{ by Taylor's theorem.}$$

Setting $\partial E/\partial \theta_e = 0$ (to find θ_e) gives

$$\sum_{n>0} a_n (n\omega x + \phi_n - \theta_e) \approx 0,$$
$$\sum_{n>0} a_n (n\omega x + \phi_n) - \sum_{n>0} a_n \theta_e \approx 0,$$
$$\theta_e \approx \frac{\sum_{n>0} a_n (n\omega x + \phi_n)}{\sum_{n>0} a_n} = \theta_r.$$

THEOREM 4. *The local energy peak location x_e is approximately equal to the least phase deviation location x_r if all harmonics' phases $(n\omega x + \phi_n)$ are close to θ_e. (That is, $x_e \approx x_r$ if $n\omega x + \phi_n - \theta_e \approx 0$.)*

PROOF. From (2.5),

$$E(x) = \sum_{n>0} a_n \cos(n\omega x + \phi_n - \theta_e)$$
$$\approx \sum_{n>0} a_n \cos(n\omega x + \phi_n - \theta_r) \quad \text{if } n\omega x + \phi_n - \theta_e \approx 0 \text{ by Theorem 3.}$$

Hence

$$\frac{\partial E}{\partial x} \approx \sum_{n>0} \left[a_n \sin(n\omega x + \phi_n - \theta_r)(n\omega - \frac{\partial \theta_r}{\partial x}) \right]$$
$$\approx \sum_{n>0} \left[a_n (n\omega x + \phi_n - \theta_r)(n\omega - \frac{\partial \theta_r}{\partial x}) \right] \quad \text{if } n\omega x + \phi_n - \theta_r \approx 0.$$

Setting $\partial E/\partial x = 0$ (to find x_e) gives

$$\sum_{n>0} \left[a_n (n\omega x_e + \phi_n - \theta_r)(n\omega - \frac{\partial \theta_r}{\partial x}) \right] \approx 0.$$

https://doi.org/10.1017/S0334270000012406 Published online by Cambridge University Press

But from (3.2) and (3.3)

$$\sum_{n>0}\left[a_n(n\omega x_r+\phi_n-\theta_r)(n\omega-\frac{\partial\theta_r}{\partial x})\right]=0.$$

Therefore $x_e \approx x_r$.

5. Numerical examples

Some numerical examples are given below to illustrate the similarities and the differences in feature locations (x_e and x_r) and phase angles (θ_e and θ_r) calculated using the local energy model and the weighted least-square method.

A generalised trapezoidal waveform is used. The waveform has zero dc and a peak to peak amplitude value 0.25. This value of peak-peak amplitude is chosen so that the curves of the luminance function ($f(x)$), the local energy ($E(x)$) and the phase deviation function ($r(x)$) can be plotted with clear details on the same scale. The waveform occupies one periodic cycle (0 to 2π) within the given frame of 257-pixels wide, and the gradient of the ramp is determined by a ratio R which is equal to the width of the ramp over the width of the plateau.

In Case 1, $R = 1$. The locations and phase angles of a feature near the point where the plateau meets the ramp are measured. The illusory features observed at the location are also known as Mach bands [13].

In Case 2, $R \approx 0$, and the slope of the ramp portion is near infinity. The feature points at the two ends of a ramp merge into a step feature, also called an edge.

In Case 3, $R \approx \infty$. The upper and lower plateau portions of a trapezoid are reduced to zero width, and the result is a sawtooth waveform where the feature points at the two ends of a plateau are merged together.

In Case 4, R is set to 1, but only the lowest nine positive and lowest nine negative frequency components of the luminance function are retained. What is being examined is a smoothed trapezoid.

As a last example (Case 5), a waveform of the least number of frequency components that exhibits a difference in θ_e and θ_r is used. Three frequency components are needed. (However, not every three-component waveform has a difference in θ_e and θ_r.)

Only the first global peak of the local energy function and the first global phase deviation minimum from the left of the waveform are tabulated and marked on the graphs as illustrations. (More peaks and minima exist at symmetrical locations towards the right of the marked points.)

https://doi.org/10.1017/S0334270000012406 Published online by Cambridge University Press

Case 1:

Suppose we are given a spatially generated trapezoidal waveform with unit R (the ramp width to plateau width ratio).

The spatially generated waveform is fast-Fourier transformed to get the necessary a_n and ϕ_n ($\omega = 2\pi$). The results are shown below in Table 1, and illustrated in Figure 1.

TABLE 1. Comparison between (x_e, θ_e) and (x_r, θ_r)

Local energy		**Weighted least-square**	
location ωx_e	23.08°	location ωx_r	22.98°
phase angle θ_e	39.04°	phase angle θ_r	36.00°
energy E at ωx_e	0.156984	least-square r at ωx_r	0.026213
energy E at $\omega x_e - 1°$	0.156034	least-square r at $\omega x_r - 1°$	0.028207
energy E at $\omega x_e + 1°$	0.156798	least-square r at $\omega x_r + 1°$	0.027189

Note: $x_e \neq x_r$ and $\theta_e \neq \theta_r$. Components' phases are only maximally (not perfectly) congruent at x_r.

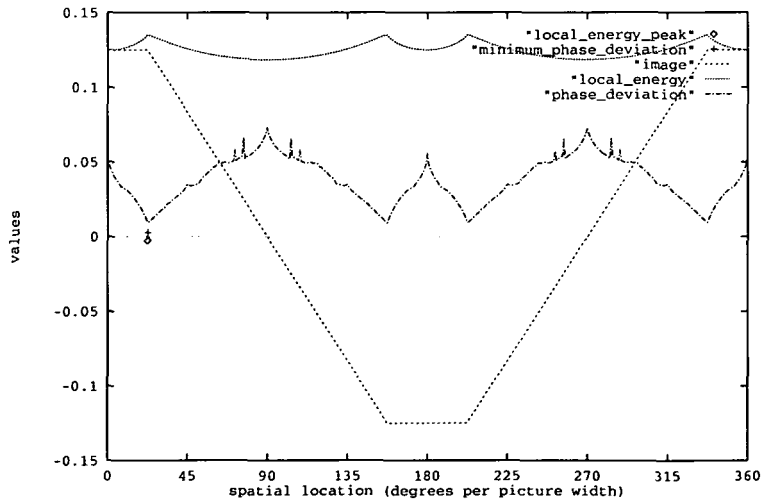

FIGURE 1. Example: a trapezoidal waveform

At this juncture, it is worth mentioning an interesting observation: at the 'smoothest' parts of the luminance function (at the middle of the ramp and the middle of the

https://doi.org/10.1017/S0334270000012406 Published online by Cambridge University Press

plateau), the local energy is minimum and the phase deviation function is maximum. This is the duality of feature definition: if the maximum of the local energy is defined as a feature point, then the minimum of the same should indicate a featureless point. A similar behaviour can be observed in the phase deviation function.

Case 2:

Suppose we are given a spatially generated square waveform by setting R to $\frac{1}{129}$.

The spatially generated waveform is fast-fourier transformed to get the necessary a_n and ϕ_n ($\omega = 2\pi$). The results are shown below in Table 2 and illustrated in Figure 2.

TABLE 2. Comparison between (x_e, θ_e) and (x_r, θ_r)

Local energy		**Weighted least-square**	
location ωx_e	90.00°	location ωx_r	90.00°
phase angle θ_e	90.00°	phase angle θ_r	90.00°
energy E at ωx_e	0.451270	least-square r at ωx_r	0.000000
energy E at $\omega x_e - 1°$	0.418383	least-square r at $\omega x_r - 1°$	0.016245
energy E at $\omega x_e + 1°$	0.418383	least-square r at $\omega x_r + 1°$	0.016245

Note: All component phases are perfectly congruent at x_r (can be seen from $r = 0.000000$ at x_r) results in $x_e = x_r$ and $\theta_e = \theta_r$.

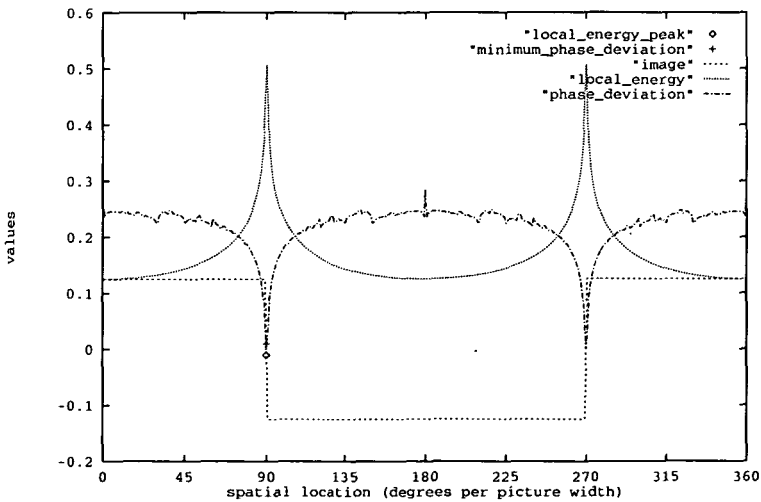

FIGURE 2. Example: a square waveform

https://doi.org/10.1017/S0334270000012406 Published online by Cambridge University Press

Case 3:

Suppose we are given a spatially generated sawtooth waveform by setting R to a large number, say 999999. The spatially generated waveform is fast-fourier transformed to get the necessary a_n and ϕ_n ($\omega = 2\pi$). The results are shown below in Table 3 and illustrated in Figure 3.

TABLE 3. Comparison between (x_e, θ_e) and (x_r, θ_r)

Local energy		**Weighted least-square**	
location ωx_e	90.00°	location ωx_r	90.00°
phase angle θ_e	180.00°	phase angle θ_r	180.00°
energy E at ωx_e	0.125000	least-square r at ωx_r	0.000000
energy E at $\omega x_e - 1°$	0.123061	least-square r at $\omega x_r - 1°$	0.003714
energy E at $\omega x_e + 1°$	0.123061	least-square r at $\omega x_r + 1°$	0.003714

Note: All component phases are perfectly congruent at x_r (can be seen from $r = 0.000000$ at x_r) resulting in $x_e = x_r$ and $\theta_e = \theta_r$.

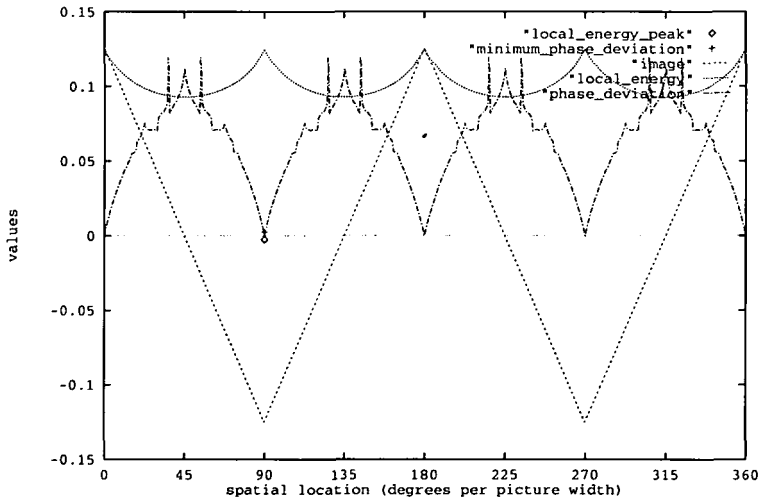

FIGURE 3. Example: a sawtooth waveform

Case 4:

This waveform consists of the lowest nine positive and lowest nine negative frequency components of a trapezoid of $R = 1$. The result is a smoothed trapezoid.

https://doi.org/10.1017/S0334270000012406 Published online by Cambridge University Press

Given

$$f(x) = \sum_{n=1}^{9} a_n \cos(n\omega x + \phi_n), \omega = 2\pi,$$

$$\begin{pmatrix} a_1 & \phi_1 \\ a_2 & \phi_2 \\ a_3 & \phi_3 \\ a_4 & \phi_4 \\ a_5 & \phi_5 \\ a_6 & \phi_6 \\ a_7 & \phi_7 \\ a_8 & \phi_8 \\ a_9 & \phi_9 \end{pmatrix} = \begin{pmatrix} 0.071703 & -23.198163° \\ 0.000000 & 0.000000° \\ 0.008018 & 110.405516° \\ 0.000000 & 0.000000° \\ 0.002924 & 64.009190° \\ 0.000000 & 0.000000° \\ 0.001521 & -162.387166° \\ 0.000000 & 0.000000° \\ 0.000944 & 151.216522° \end{pmatrix},$$

and note that $a_n = a_{-n}$, $\phi_n = -\phi_{-n}$. The results are shown below in Table 4 and illustrated in Figure 4.

TABLE 4. Comparison between (x_e, θ_e) and (x_r, θ_r)

Local energy		**Weighted least-square**	
location ωx_e	80.15°	location ωx_r	78.83°
phase angle θ_e	53.52°	phase angle θ_r	51.09°
energy E at ωx_e	0.156817	least-square r at ωx_r	0.017876
energy E at $\omega x_e - 1°$	0.156791	least-square r at $\omega x_r - 1°$	0.017938
energy E at $\omega x_e + 1°$	0.156793	least-square r at $\omega x_r + 1°$	0.017938

Note that $x_e \neq x_r$ and $\theta_e \neq \theta_r$. Components' phases are only maximally (not perfectly) congruent at x_r.

Case 5:

In this case, a waveform that has no perfect phase congruency (that is, $r \neq 0$ at x_r) will be examined. Such a waveform must consist of at least three harmonics.

Given

$$f(x) = 0.25\cos(\omega x) - 0.25\cos(3\omega x) - 0.25\cos(5\omega x)$$
$$= \sum_{n=1}^{3} a_n \cos(n\omega x + \phi_n),$$

where

$$\omega = 2\pi,$$
$$a_1 = 0.125, a_2 = 0.000, a_3 = 0.125, a_4 = 0.000, a_5 = 0.125,$$
$$\phi_1 = 0°, \phi_2 = 0°, \phi_3 = 180°, \phi_4 = 0°, \phi_5 = 180°.$$

https://doi.org/10.1017/S0334270000012406 Published online by Cambridge University Press

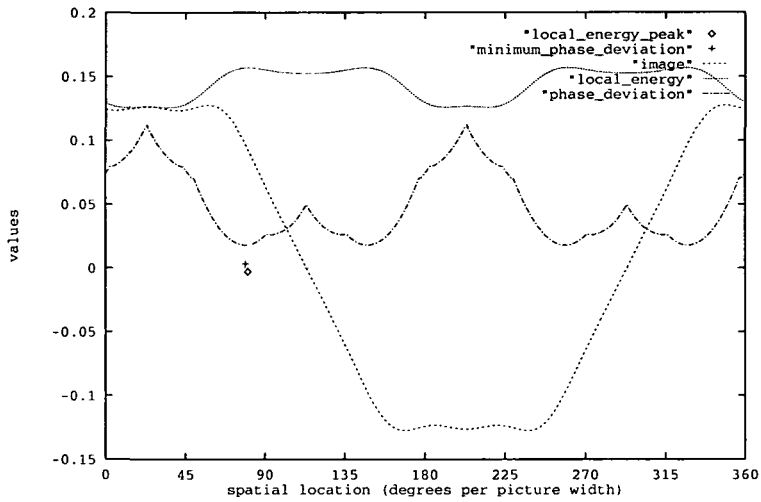

FIGURE 4. Example: a waveform synthesized from the first 9 positive and negative harmonics of a trapezoid

The results are illustrated below.

TABLE 5. Comparison between (x_e, θ_e) and (x_r, θ_r)

Local energy		**Weighted least-square**	
location ωx_e	45.00°	location ωx_r	45.00°
phase angle θ_e	18.43°	phase angle θ_r	15.00°
energy E at ωx_e	0.279509	least-square r at ωx_r	0.055556
energy E at $\omega x_e - 1°$	0.279372	least-square r at $\omega x_r - 1°$	0.055638
energy E at $\omega x_e + 1°$	0.279372	least-square r at $\omega x_r + 1°$	0.055638

Note that $x_e = x_r$ but $\theta_e \neq \theta_r$. Components' phases are only maximally (not perfectly) congruent at x_r.

6. Orientation invariance

In this section, the hypothesis that the location of the local maxima of local energy is invariant to the orientation of the orthogonal bases of operation with respect to the image is examined. In common practice, the set of peaks detected from one

https://doi.org/10.1017/S0334270000012406 Published online by Cambridge University Press

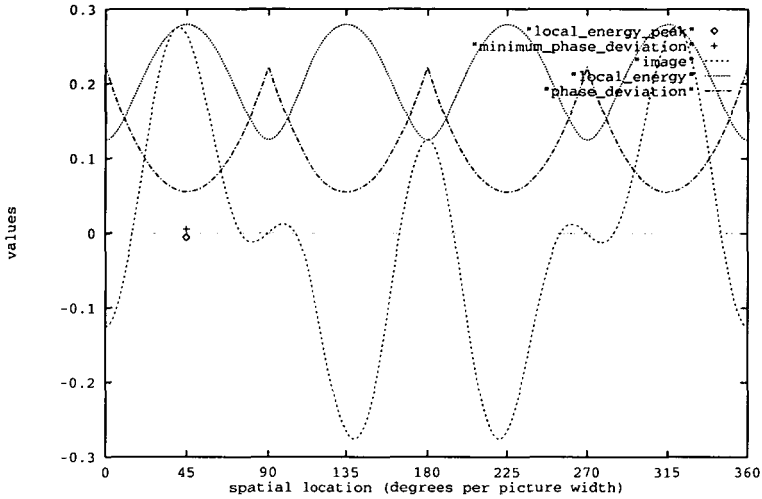

FIGURE 5. Example: a 3-harmonic waveform having no perfect phase congruency

direction is simply united (that is, logical OR operation) with those found in the other orthogonal direction to form a so-called two-dimensional feature map of an image. In the following paragraphs, it will be shown that in order to obtain invariance in the detected locations with respect to the orientation of the applied operator, there is a necessary condition of zero-gradient in the local energy in *both* directions at a peak point (§6.1). That is, peak detection in one direction cannot be carried out regardless of the local energy gradient found in the other direction. (Usual second derivative tests can be carried out but are omitted in this paper for simplicity.) The same necessary condition applies to feature point detection using the weighted least-square criterion, in which case a minimum in one direction must be matched with a zero gradient in the other direction (§6.2).

6.1. Consistency in peak point in the local energy model. Assume that a peak is present in a two-dimensional zero-dc image. Since the Hilbert transform does not exist for a general two-dimensional image, without loss of generality, one can further restrict the image to be one of positive frequency components only. Then, using the horizontal and vertical directions of the image as the axes for x and y, and centering the origin of the coordinates at the said peak, the image can be expressed as

$$f(x, y) = \sum_{m,n>0} a_{m,n} \cos(m\omega_x x + n\omega_y y + \phi_{m,n}), \tag{6.1}$$

https://doi.org/10.1017/S0334270000012406 Published online by Cambridge University Press

and the Hilbert transform of the image is

$$h(x, y) = -\sum_{m,n>0} a_{m,n} \sin(m\omega_x x + n\omega_y y + \phi_{m,n}). \tag{6.2}$$

The local energy function of the image (ignoring the scaling factor of $\frac{1}{2}$ in (2.3)) is

$$E(x, y) = \left(\left[\sum_{m,n>0} a_{m,n} \cos(m\omega_x x + n\omega_y y + \phi_{m,n}) \right]^2 + \left[\sum_{m,n>0} a_{m,n} \sin(m\omega_x x + n\omega_y y + \phi_{m,n}) \right]^2 \right)^{1/2}. \tag{6.3}$$

Let the square of $E(x, y)$ be $Z(x, y)$. In usual peak searching, $Z(x, y)$ is maximised in the horizontal and the vertical directions separately (by setting $\partial Z/\partial x$ and $\partial Z/\partial y$ separately to zero together with second derivative tests), and the union taken the set of peak locations found in the two directions. We have

$$Z(x, y) = \left[\sum_{m,n>0} a_{m,n} \cos(m\omega_x x + n\omega_y y + \phi_{m,n}) \right]^2 + \left[\sum_{m,n>0} a_{m,n} \sin(m\omega_x x + n\omega_y y + \phi_{m,n}) \right]^2, \tag{6.4}$$

so that

$$\frac{\partial Z}{\partial x} = -2 \left[\sum_{m,n>0} a_{m,n} \cos(m\omega_x x + n\omega_y y + \phi_{m,n}) \right] \times \left[\sum_{m,n>0} a_{m,n} m\omega_x \sin(m\omega_x x + n\omega_y y + \phi_{m,n}) \right] + 2 \left[\sum_{m,n>0} a_{m,n} \sin(m\omega_x x + n\omega_y y + \phi_{m,n}) \right] \times \left[\sum_{m,n>0} a_{m,n} m\omega_x \cos(m\omega_x x + n\omega_y y + \phi_{m,n}) \right] \tag{6.5}$$

and

$$\frac{\partial Z}{\partial y} = -2 \left[\sum_{m,n>0} a_{m,n} \cos(m\omega_x x + n\omega_y y + \phi_{m,n}) \right]$$

https://doi.org/10.1017/S0334270000012406 Published online by Cambridge University Press

$$\times \left[\sum_{m,n>0} a_{m,n} n\omega_y \sin(m\omega_x x + n\omega_y y + \phi_{m,n}) \right]$$
$$+ 2 \left[\sum_{m,n>0} a_{m,n} \sin(m\omega_x x + n\omega_y y + \phi_{m,n}) \right]$$
$$\times \left[\sum_{m,n>0} a_{m,n} n\omega_y \cos(m\omega_x x + n\omega_y y + \phi_{m,n}) \right]. \tag{6.6}$$

At the origin $(x, y) = (0, 0)$,

$$\frac{\partial Z}{\partial x}_{(x,y)=(0,0)} = -2 \left[\sum_{m,n>0} a_{m,n} \cos(\phi_{m,n}) \right] \left[\sum_{m,n>0} a_{m,n} m\omega_x \sin(\phi_{m,n}) \right]$$
$$+ 2 \left[\sum_{m,n>0} a_{m,n} \sin(\phi_{m,n}) \right] \left[\sum_{m,n>0} a_{m,n} m\omega_x \cos(\phi_{m,n}) \right] \tag{6.7}$$

and

$$\frac{\partial Z}{\partial y}_{(x,y)=(0,0)} = -2 \left[\sum_{m,n>0} a_{m,n} \cos(\phi_{m,n}) \right] \left[\sum_{m,n>0} a_{m,n} n\omega_y \sin(\phi_{m,n}) \right]$$
$$+ 2 \left[\sum_{m,n>0} a_{m,n} \sin(\phi_{m,n}) \right] \left[\sum_{m,n>0} a_{m,n} n\omega_y \cos(\phi_{m,n}) \right]. \tag{6.8}$$

Next, consider an anti-clockwise rotation of axes about the origin by an angle θ. Let the units of measurement along the rotated axes be u and v. By simple geometry

$$x = u\cos(\theta) - v\sin(\theta) \tag{6.9}$$

and

$$y = u\sin(\theta) + v\cos(\theta). \tag{6.10}$$

Substituting (6.9) and (6.10) into (6.4) gives

$$Z(x, y) = \left\{ \sum_{m,n>0} a_{m,n} \cos\left[m\omega_x (u\cos\theta - v\sin\theta) \right.\right.$$
$$\left.\left. + n\omega_y (u\sin\theta + v\cos\theta) + \phi_{m,n} \right] \right\}^2$$

https://doi.org/10.1017/S0334270000012406 Published online by Cambridge University Press

$$+\left\{\sum_{m,n>0} a_{m,n}\sin\left[m\omega_x(u\cos\theta - v\sin\theta) + n\omega_y(u\sin\theta + v\cos\theta) + \phi_{m,n}\right]\right\}^2, \tag{6.11}$$

$$\frac{\partial Z}{\partial u} = -2\left\{\sum_{m,n>0} a_{m,n}\cos[m\omega_x(u\cos\theta - v\sin\theta) + n\omega_y(u\sin\theta + v\cos\theta) + \phi_{m,n}]\right\}$$
$$\times\left\{\sum_{m,n>0} a_{m,n}(m\omega_x\cos\theta + n\omega_y\sin\theta)\right.$$
$$\left.\sin[m\omega_x(u\cos\theta - v\sin\theta) + n\omega_y(u\sin\theta + v\cos\theta) + \phi_{m,n}]\right\}$$
$$+2\left\{\sum_{m,n>0} a_{m,n}\sin[m\omega_x(u\cos\theta - v\sin\theta) + n\omega_y(u\sin\theta + v\cos\theta) + \phi_{m,n}]\right\}$$
$$\times\left\{\sum_{m,n>0} a_{m,n}(m\omega_x\cos\theta + n\omega_y\sin\theta)\right.$$
$$\left.\cos[m\omega_x(u\cos\theta - v\sin\theta) + n\omega_y(u\sin\theta + v\cos\theta) + \phi_{m,n}]\right\}, \tag{6.12}$$

$$\frac{\partial Z}{\partial v} = -2\left\{\sum_{m,n>0} a_{m,n}\cos[m\omega_x(u\cos\theta - v\sin\theta) + n\omega_y(u\sin\theta + v\cos\theta) + \phi_{m,n}]\right\}$$
$$\times\left\{\sum_{m,n>0} a_{m,n}(n\omega_y\cos\theta - m\omega_x\sin\theta)\right.$$
$$\left.\sin[m\omega_x(u\cos\theta - v\sin\theta) + n\omega_y(u\sin\theta + v\cos\theta) + \phi_{m,n}]\right\}$$
$$+2\left\{\sum_{m,n>0} a_{m,n}\sin[m\omega_x(u\cos\theta - v\sin\theta) + n\omega_y(u\sin\theta + v\cos\theta) + \phi_{m,n}]\right\}$$
$$\times\left\{\sum_{m,n>0} a_{m,n}(n\omega_y\cos\theta - m\omega_x\sin\theta)\right.$$
$$\left.\cos[m\omega_x(u\cos\theta - v\sin\theta) + n\omega_y(u\sin\theta + v\cos\theta) + \phi_{m,n}]\right\}. \tag{6.13}$$

https://doi.org/10.1017/S0334270000012406 Published online by Cambridge University Press

At the origin (where a peak is supposed to exist), $(u, v) = (0, 0)$, (6.12) and (6.13) give

$$\begin{aligned}
&\frac{\partial Z}{\partial u}_{(u,v)=(0,0)} \\
&\quad = -2\left\{\sum_{m,n>0} a_{m,n}\cos[\phi_{m,n}]\right\}\left\{\sum_{m,n>0} a_{m,n}(m\omega_x\cos\theta + n\omega_y\sin\theta)\sin[\phi_{m,n}]\right\} \\
&\qquad + 2\left\{\sum_{m,n>0} a_{m,n}\sin[\phi_{m,n}]\right\}\left\{\sum_{m,n>0} a_{m,n}(m\omega_x\cos\theta + n\omega_y\sin\theta)\cos[\phi_{m,n}]\right\} \\
&\quad = -2\left\{\sum_{m,n>0} a_{m,n}\cos[\phi_{m,n}]\right\}\left\{\sum_{m,n>0} a_{m,n}m\omega_x\cos\theta\sin[\phi_{m,n}]\right\} \\
&\qquad + 2\left\{\sum_{m,n>0} a_{m,n}\sin[\phi_{m,n}]\right\}\left\{\sum_{m,n>0} a_{m,n}m\omega_x\cos\theta\cos[\phi_{m,n}]\right\} \\
&\qquad - 2\left\{\sum_{m,n>0} a_{m,n}\cos[\phi_{m,n}]\right\}\left\{\sum_{m,n>0} a_{m,n}n\omega_y\sin\theta\sin[\phi_{m,n}]\right\} \\
&\qquad + 2\left\{\sum_{m,n>0} a_{m,n}\sin[\phi_{m,n}]\right\}\left\{\sum_{m,n>0} a_{m,n}n\omega_y\sin\theta\cos[\phi_{m,n}]\right\} \\
&\quad = \cos\theta\frac{\partial Z}{\partial x}_{(x,y)=(0,0)} + \sin\theta\frac{\partial Z}{\partial y}_{(x,y)=(0,0)} \qquad (6.14)
\end{aligned}$$

and

$$\begin{aligned}
&\frac{\partial Z}{\partial v}_{(u,v)=(0,0)} \\
&\quad = -2\left\{\sum_{m,n>0} a_{m,n}\cos[\phi_{m,n}]\right\}\left\{\sum_{m,n>0} a_{m,n}(n\omega_y\cos\theta - m\omega_x\sin\theta)\sin[\phi_{m,n}]\right\} \\
&\qquad + 2\left\{\sum_{m,n>0} a_{m,n}\sin[\phi_{m,n}]\right\}\left\{\sum_{m,n>0} a_{m,n}(n\omega_y\cos\theta - m\omega_x\sin\theta)\cos[\phi_{m,n}]\right\} \\
&\quad = -2\left\{\sum_{m,n>0} a_{m,n}\cos[\phi_{m,n}]\right\}\left\{\sum_{m,n>0} a_{m,n}n\omega_y\cos\theta\sin[\phi_{m,n}]\right\} \\
&\qquad + 2\left\{\sum_{m,n>0} a_{m,n}\sin[\phi_{m,n}]\right\}\left\{\sum_{m,n>0} a_{m,n}n\omega_y\cos\theta\cos[\phi_{m,n}]\right\} \\
&\qquad + 2\left\{\sum_{m,n>0} a_{m,n}\cos[\phi_{m,n}]\right\}\left\{\sum_{m,n>0} a_{m,n}m\omega_x\sin\theta\sin[\phi_{m,n}]\right\}
\end{aligned}$$

https://doi.org/10.1017/S0334270000012406 Published online by Cambridge University Press

$$-2\left\{\sum_{m,n>0} a_{m,n}\sin[\phi_{m,n}]\right\}\left\{\sum_{m,n>0} a_{m,n}m\omega_x \sin\theta\cos[\phi_{m,n}]\right\}$$
$$= -\sin\theta\frac{\partial Z}{\partial x}_{(x,y)=(0,0)} + \cos\theta\frac{\partial Z}{\partial y}_{(x,y)=(0,0)}. \tag{6.15}$$

For $\partial Z/\partial u$ or $\partial Z/\partial v$ ((6.14), (6.15)) to be zero at the origin (where a feature lies) regardless of θ, $\partial Z/\partial x$ *and* (not *or*) $\partial Z/\partial y$ must be *both* zero. In other words, if the feature location detected in one coordinate system is to remain invariant with respect to the axes, the gradient in both directions must be zero before the point of interest can be tested further as a feature point. The test of sufficiency using second derivatives can be carried out as normal.

6.2. Consistency of minimum point in phase deviation using the weighted least-square criterion. As before, the same $x - y$ coordinates whose origin centres on a feature point are used. In this case, however, the feature point is a location where there is a minimum in the phase deviation function $r(x, y)$ which is defined as

$$r(x, y) = \frac{\sum_{m>0}\sum_{n>0} a_{m,n}(m\omega_x x + n\omega_y y + \phi_{m,n} - \theta_r)^2}{\pi^2 \sum_{m>0}\sum_{n>0} a_{m,n}}, \tag{6.16}$$

where $m\omega_x x + n\omega_y y + \phi_{m,n} - \theta_r$ assumes values in the principal range of $(-\pi, \pi]$ and

$$\theta_r = \frac{\sum_{m>0}\sum_{n>0} a_{m,n}(m\omega_x x + n\omega_y y + \phi_{m,n})}{\sum_{m>0}\sum_{n>0} a_{m,n}}. \tag{6.17}$$

Considering the gradient $\partial r/\partial x$ and $\partial r/\partial y$,

$$\frac{\partial r}{\partial x} = \frac{2}{\pi^2 \sum_{m>0}\sum_{n>0} a_{m,n}} \sum_{m>0}\sum_{n>0} a_{m,n}(m\omega_x x + n\omega_y y + \phi_{m,n} - \theta_r)\left(m\omega_x - \frac{\partial\theta_r}{\partial x}\right). \tag{6.18}$$

Let

$$M_1 = \frac{\sum_{m>0}\sum_{n>0} a_{m,n}m}{\sum_{m>0}\sum_{n>0} a_{m,n}}, \qquad M_2 = \frac{\sum_{m>0}\sum_{n>0} a_{m,n}n}{\sum_{m>0}\sum_{n>0} a_{m,n}} \quad \text{and} \quad N = \frac{\sum_{m>0}\sum_{n>0} a_{m,n}\phi_{m,n}}{\sum_{m>0}\sum_{n>0} a_{m,n}}.$$

Then,

$$\theta_r = \omega_x x M_1 + \omega_y y M_2 + N, \qquad \frac{\partial\theta_r}{\partial x} = \omega_x M_1.$$

https://doi.org/10.1017/S0334270000012406 Published online by Cambridge University Press

Therefore,

$$\frac{\partial r}{\partial x} = \frac{2\sum_{m,n>0} a_{m,n}(m\omega_x x + n\omega_y y + \phi_{m,n} - \omega_x x M_1 - \omega_y y M_2 - N)(m\omega_x - \omega_x M_1)}{\pi^2 \sum_{m>0}\sum_{n>0} a_{m,n}}. \tag{6.19}$$

Similarly,

$$\frac{\partial r}{\partial y} = \frac{2\sum_{m,n>0} a_{m,n}(m\omega_x x + n\omega_y y + \phi_{m,n} - \omega_x x M_1 - \omega_y y M_2 - N)(n\omega_y - \omega_y M_2)}{\pi^2 \sum_{m>0}\sum_{n>0} a_{m,n}}. \tag{6.20}$$

At the origin, $(x, y) = (0, 0)$, the gradients are

$$\frac{\partial r}{\partial x}_{(x,y)=(0,0)} = \frac{2}{\pi^2 \sum_{m,n>0} a_{m,n}} \sum_{m,n>0} a_{m,n}(\phi_{m,n} - N)(m\omega_x - \omega_x M_1) \tag{6.21}$$

and

$$\frac{\partial r}{\partial y}_{(x,y)=(0,0)} = \frac{2}{\pi^2 \sum_{m,n>0} a_{m,n}} \sum_{m,n>0} a_{m,n}(\phi_{m,n} - N)(n\omega_y - \omega_y M_2). \tag{6.22}$$

Next, consider the rotated coordinates (u, v) and the substitution of (6.9) and (6.10) into (6.16) and (6.17) we have

$$r(u, v) = \frac{\sum_{m,n>0} a_{m,n}(m\omega_x(u\cos\theta - v\sin\theta) + n\omega_y(u\sin\theta + v\cos\theta) + \phi_{m,n} - \theta_r)^2}{\pi^2 \sum_{m>0}\sum_{n>0} a_{m,n}}, \tag{6.23}$$

where $m\omega_x(u\cos\theta - v\sin\theta) + n\omega_y(u\sin\theta + v\sin\theta) + \phi_{m,n} - \theta_r$ assumes values in the principal range of $(-\pi, \pi]$.

Also

$$\theta_r = \frac{\sum_{m,n>0} a_{m,n}(m\omega_x(u\cos\theta - v\sin\theta) + n\omega_y(u\sin\theta + v\cos\theta) + \phi_{m,n})}{\sum_{m>0}\sum_{n>0} a_{m,n}}$$

$$= \omega_x(u\cos\theta - v\sin\theta)M_1 + \omega_y(u\sin\theta + v\cos\theta)M_2 + N, \tag{6.24}$$

$$\frac{\partial\theta_r}{\partial u} = \omega_x M_1\cos\theta + \omega_y M_2\sin\theta, \tag{6.25}$$

https://doi.org/10.1017/S0334270000012406 Published online by Cambridge University Press

$$\frac{\partial \theta_r}{\partial v} = -\omega_x M_1 \sin\theta + \omega_y M_2 \cos\theta. \tag{6.26}$$

Substituting (6.25) and (6.26) into the expressions for $\partial r/\partial u$ and $\partial r/\partial v$ gives

$$\frac{\partial r}{\partial u} = \frac{2}{\pi^2 \sum_{m,n>0} a_{m,n}} \sum_{m,n>0} \Big(a_{m,n}(m\omega_x(u\cos\theta - v\sin\theta) + n\omega_y(u\sin\theta + v\cos\theta) + \phi_{m,n} - \theta_r)(m\omega_x\cos\theta + n\omega_y\sin\theta - \frac{\partial \theta_r}{\partial u}) \Big),$$

$$\begin{aligned}
\frac{\partial r}{\partial u}_{(u,v)=(0,0)} &= \frac{2}{\pi^2 \sum_{m,n>0} a_{m,n}} \sum_{m,n>0} a_{m,n}(\phi_{m,n} - \theta_r) \\
&\qquad \times (m\omega_x\cos\theta + n\omega_y\sin\theta - \omega_x M_1\cos\theta - \omega_y M_2\sin\theta) \\
&= \frac{2}{\pi^2 \sum_{m,n>0} a_{m,n}} \sum_{m,n>0} a_{m,n}(\phi_{m,n} - N)(m\omega_x - \omega_x M_1)\cos\theta \\
&\quad + \frac{2}{\pi^2 \sum_{m,n>0} a_{m,n}} \sum_{m,n>0} a_{m,n}(\phi_{m,n} - N)(n\omega_y - \omega_y M_2)\sin\theta \\
&= \cos\theta \frac{\partial r}{\partial x}_{(x,y)=(0,0)} + \sin\theta \frac{\partial r}{\partial y}_{(x,y)=(0,0)},
\end{aligned} \tag{6.27}$$

and

$$\begin{aligned}
\frac{\partial r}{\partial v} &= \frac{2}{\pi^2 \sum_{m>0}\sum_{n>0} a_{m,n}} \\
&\quad \times \sum_{m,n>0} a_{m,n}(m\omega_x(u\cos\theta - v\sin\theta) + n\omega_y(u\sin\theta + v\cos\theta) + \phi_{m,n} - \theta_r) \\
&\quad \times \left(-m\omega_x\sin\theta + n\omega_y\cos\theta - \frac{\partial \theta_r}{\partial v} \right),
\end{aligned}$$

https://doi.org/10.1017/S0334270000012406 Published online by Cambridge University Press

$$\frac{\partial r}{\partial v}_{(u,v)=(0,0)}$$

$$= \frac{2\sum_{m,n>0} a_{m,n}(\phi_{m,n} - \theta_r)(-m\omega_x \sin\theta + n\omega_y \cos\theta + \omega_x M_1 \sin\theta - \omega_y M_2 \cos\theta)}{\pi^2 \sum_{m>0}\sum_{n>0} a_{m,n}}$$

$$= \frac{2}{\pi^2 \sum_{m>0}\sum_{n>0} a_{m,n}} \sum_{m>0}\sum_{n>0} a_{m,n}(\phi_{m,n} - N)(-m\omega_x + \omega_x M_1)\sin\theta$$

$$+ \frac{2}{\pi^2 \sum_{m>0}\sum_{n>0} a_{m,n}} \sum_{m>0}\sum_{n>0} a_{m,n}(\phi_{m,n} - N)(n\omega_y - \omega_y M_2)\cos\theta$$

$$= -\sin\theta \frac{\partial r}{\partial x}_{(x,y)=(0,0)} + \cos\theta \frac{\partial r}{\partial y}_{(x,y)=(0,0)}. \tag{6.28}$$

Again, for $\partial r/\partial u$ or $\partial r/\partial v$ ((6.27), (6.28)) to be zero at the origin (where a feature lies) regardless of θ, $\partial r/\partial x$ *and* (not *or*) $\partial r/\partial v$ must *both* be zero. (Usual second derivatives test can be worked out and also note that (6.27) and (6.28) have the same form as (6.14) and (6.15).)

In summary, if a feature point is defined at the minimum phase deviation point (in the weighted least-square sense), and if the detected location is to be invariant to the arbitrary orientation of the coordinate axes with respect to the image, then it is necessary to check for zero gradient in *both* axis directions when determining a feature point in one direction.

7. Conclusion

We have shown that features detected by searching for the local energy peaks or by looking for minimum phase deviation in the weighted least-square sense can differ slightly in locations and phase angles. If the harmonics' phases are perfectly congruent, as in the case of a perfect step or sawtooth (roof) luminance function (Cases 2 and 3 in Section 2.5), there is no difference between the two methods in location and in phase angle. If, however, the harmonics' phases are only maximally (not perfectly) congruent, as in the case of a trapezoidal luminance function or combinations of steps and roof profiles, small differences in the order of a few degrees per picture width can exist in locations and phase angles calculated by the two methods. This is due to the fact that the local energy method is a Taylor-approximation of the weighted least-square method in measuring phase congruency.

The consistency in the detected feature location with respect to an arbitrary set of orientations of the applied energy operator has also been examined. We showed

https://doi.org/10.1017/S0334270000012406 Published online by Cambridge University Press

that while determining a local energy peak in one direction (say, the x-direction) as a feature point, it is important to check that the gradient of the local energy in the orthogonal direction (the y-direction) is also zero, though it need not be a peak in the y-direction at the same time (as in the case of a roof profile in the x-direction with a constant luminance in the y-direction). However, if one decides that a roof profile in the x-direction with a gradual increase in luminance in the y-direction is to contain features at peaks of the roof points, then *a priori* knowledge about the feature line orientation is needed to apply the local energy operator correctly in a direction perpendicular to the feature line. Any other orientation of coordinate system will give inconsistent results on feature point locations.

A similar necessary condition applies to feature point detection using the weighted least-square phase deviation function. A zero-gradient condition in the deviation function in the orthogonal (y) direction must be met when deciding whether the minimum point in phase deviation in the current (x) direction is a feature point (and *vice versa*).

Acknowledgements

This research was funded by the ARC.

References

[1] Y. K. Aw, R. A. Owens and J. Ross, "Feature detection and classification by tuned-neurons", in *Proc. 4th Autralian Joint Conference on Artificial Intelligence, 21th-23rd, Nov 1990, Perth*, (1990) 291–303.

[2] Y. K. Aw, R. A. Owens and J. Ross, "Image compression and reconstruction using a 1-d feature catalogue", in *Proc. of the Second European Conference on Computer Vision, Santa Margherita Ligure, Italy, May 1992*, (1992) 749–753.

[3] Y. K. Aw, R. A. Owens and J. Ross, "Learning features in natural images", in *Proc. of the IEEE international conference on Neural Network Applications to Signal Processing*, (1993).

[4] Y. K. Aw, R. A. Owens and J. Ross, "A catalogue of 1-D features in natural image", *J. Comp. Vision, Graph. and Im. Processing* **56** (1994) 173–181.

[5] J. F. Canny, "A computational approach to edge detection", *IEEE Trans. on PAMI* **8** (1986) 679–697.

[6] D. J. Fleet and A. D. Jepson, "Computation of component image velocity from local phase information", *Int. J. Comp. Vision* **5** (1991) 77–104.

[7] R. M. Haralick, "Edge and region analysis for digital image data", *Comp. Graph. and Im. Processing* **12** (1980) 60–73.

[8] R. M. Haralick, "Digital step edges from zero crossings of second directional derivatives", *IEEE Trans. on PAMI* **6** (1984) 58–68.

[9] P. Kovesi, "A dimensionless measure of edge significance from phase congruency calculated via wavelets", in *Procs. 1st New Zealand Conf. on Image and Vision Computing, Auckland*, (1994) 87–94.

[10] D. Marr and E. Hildreth, "Theory of edge detection", *Proc. R. Soc. London Ser. B* **207** (1980) 187–217.

[11] C. Morrone and R. A. Owens, "Feature detection from local energy", *Pattern Recognition Letters* **6** (1987) 303–313.

[12] M. C. Morrone and D. C. Burr, "A phase-dependent energy model", *Proc. R. Soc. London Ser. B* **235** (1988) 221–245.

[13] M. C. Morrone, J. Ross, D. C. Burr and R. Owens, "Mach bands are phase dependent", *Nature* **324** (1986) 250–253.

[14] A. Noble, "Morphological feature detection", in *Second Int. Conference on Comp. Vis., Dec 5-8, 1988 Florida, USA*, 112–116.

[15] Alan V. Oppenheim and Jae S. Lim, "The importance of phase in signals", *Proceedings of the IEEE* **69** (1981) 529–541.

[16] R. A. Owens, "Feature-free images", *Pattern Recognition Letters* **15** (1994) 35–44.

[17] R. A. Owens, Y. K. Aw and J. Ross, "Stable feature structure in images", in *DICTA-91, Proceedings of the conference on Digital Image Processing: Techniques and Applications* (1991) 357–364.

[18] R. A. Owens, S. Venkatesh and J. Ross, "Edge detection is a projection", *Pattern Recognition Letters* **9** (1989) 233–244.

[19] T. Peli and D. Malah, "A study of edge detection algorithms", *Comp. Graph. and Imag. Proc.* **20** (1982) 1–21.

[20] B. Robbins and R. Owens, "The 2D local energy model", Technical report 94/5, Department of Computer Science, The University of Western Australia, 1994.

[21] S. M. Smith and J. M. Brady, "SUSAN - a new approach to low level image processing", DRA Technical Report TR95SMS1b, Defence Research Agency, Farnborough, Hampshire, GU14 6TD, UK, 1994.

[22] S. Venkatesh, "A study of energy based models for the detection and classification of image features", Ph. D. Thesis, The University of Western Australia, Department of Computer Science, 1990.

[23] S. Venkatesh and R. A. Owens, "On the classification of image features", *Pattern Recognition Letters* **11** (1990) 339–349.